Human Molecular Genetics, 2008, Vol. 17, No. 17 **2703–2711**
doi:10.1093/hmg/ddn172
Advance Access published on June 19, 2008

HMSN/ACC truncation mutations disrupt brain-type creatine kinase-dependant activation of K^+/Cl^- co-transporter 3

Adèle Salin-Cantegrel[1], Masoud Shekarabi[1], Sébastien Holbert[1], Patrick Dion[1], Daniel Rochefort[1], Janet Laganière[1], Sandra Dacal[2], Pascale Hince[1], Liliane Karemera[1], Claudia Gaspar[1], Jean-Yves Lapointe[2] and Guy A. Rouleau[1,*]

[1]Centre of Excellence in Neuromics, CHUM Research Centre and the Department of Medicine, University of Montreal, Montreal, Qc, Canada, H2L 4M1 and [2]Department of Physics, University of Montreal, Montreal, Qc, Canada, H3C 3J7

Received March 3, 2008; Revised May 7, 2008; Accepted June 10, 2008

The potassium-chloride co-transporter 3 (KCC3) is mutated in hereditary motor and sensory neuropathy with agenesis of the corpus callosum (HMSN/ACC); however, the molecular mechanisms of HMSN/ACC pathogenesis and the exact role of KCC3 in the development of the nervous system remain poorly understood. The functional regulation of this transporter by protein partners is also largely unknown. Using a yeast two-hybrid approach, we discovered that the C-terminal domain (CTD) of KCC3, which is lost in most HMSN/ACC-causing mutations, directly interacts with brain-specific creatine kinase (CK-B), an ATP-generating enzyme that is also a partner of KCC2. The interaction of KCC3 with CK-B was further confirmed by *in vitro* glutathione S-transferase pull-down assay, followed by sequencing of the pulled-down complexes. In transfected cultured cells, immunofluorescence labeling showed that CK-B co-localizes with wild-type KCC3, whereas the kinase fails to interact with the inactive truncated KCC3. Finally, CK-B's inhibition by DNFB results in reduction of activity of KCC3 in functional assays using *Xenopus laevis* oocytes. This physical and functional association between the co-transporter and CK-B is, therefore, the first protein–protein interaction identified to be potentially involved in the pathophysiology of HMSN/ACC.

INTRODUCTION

Hereditary motor and sensory neuropathy with agenesis of the corpus callosum (HMSN/ACC) is an autosomal recessive severely invalidating and ultimately fatal disease. Both development and maintenance of the integrity of the nervous system are impaired, and the most striking histopathological findings include abnormal axonal migration through the brain midline and massive swelling of peripheral nerves accompanied by demyelination (1). HMSN/ACC is a monogenic disease caused by mutations in the *KCC3* gene, which codes for the potassium-chloride co-transporter 3 (KCC3) (2). Since KCC3 allows the outward transport of K^+ and Cl^- ions and subsequently water through the plasma membrane, the protein is thought to be involved in regulatory volume decrease (RVD) response and ion homeostasis (3,4). Therefore, we suspect that a complete loss of function of the transporter may account for the swollen axons observed in patients, a hallmark of HMSN/ACC pathology. However, many aspects of the disease remain to be explained.

Several topology studies reported that KCC3 is a large integral glycoprotein that contains 12 membrane-spanning domains and includes a variable N-terminal region and a large C-terminal domain (CTD) within the cytoplasm (3,5–7). Truncation of the CTD is predicted to occur in most of the HMSN/ACC mutations (8/9 mutations) (2,8,9), suggesting a key role for this part of the protein. We have so far performed functional studies of the two mutations most commonly found worldwide (2436delG, T813fsX813 and 3031C→T, R1011X), and demonstrated that: (i) a mutation in exon 18, which is found in the French-Canadian population at a high rate, truncates a third of the whole

*To whom correspondence should be addressed at: Centre of Excellence in Neuromics, CHUM Research Centre, Notre-Dame Hospital, 2099 Alexandre-de-Seve, Montreal, Qc, H2L 4M1, Canada. Tel: +1 5148908000; Fax: +1 5144127602; Email: guy.rouleau@umontreal.ca

protein and inactivates the co-transporter (2); (ii) a mutation in exon 22 produces the R1011X truncated form of KCC3 in ethnically diverse populations, and also inactivates the transporter, even if only a third of the CTD is missing (9). These data reinforce the hypothesis that the CTD in KCC3 is critical for function, possibly due to defective protein–protein interactions.

In a recent study, it was shown that the neuronal-specific KCC2, a protein involved in the determination of resting $(Cl^-)i$, interacts with brain-type creatine kinase (CK-B) via the CTD of this co-transporter (10). Using an electrophysiological approach, the authors demonstrated that CK-B activates KCC2 in their HEK293 cellular transfection model (11). It was also strongly suggested that creatine kinases play a key role in the activation of potassium-chloride co-transport in red blood cells (12). The key requirement for creatine kinases in mammalian cells, including CK-B, is primarily linked to the cytoplasmic instability of ATP: in order to shuffle energy within the cell, the inorganic phosphate (Pi) of ATP is conjugated with creatine to produce phospho-creatine. Phospho-creatine is high in energy and stable, but, contrary to ATP, its energy is unavailable for direct usage. In the nervous system, phospho-creatine is the prime substrate for CK-B, which catalyses the transfer of Pi from phospho-creatine to ADP. CK-B thus allows the production of ATP in a precisely controlled spatial and temporal manner (13).

The aims of the present study are to (i) investigate the potential interaction between CK-B and KCC3, (ii) assess the impact of this key protein–protein interaction on the function of the transporter and (iii) deduct its contribution to HMSN/ACC pathogenesis. Our findings show that KCC3 naturally occurring truncation mutations lead to a loss of interaction between the transporter and CK-B. This interaction has a major impact on the activity of the co-transporter, similar to the functional defect of HMSN/ACC truncated KCC3.

RESULTS

Yeast two-hybrid and GST pull-down assays identify CK-B as a binding partner of KCC3

The CTDs of KCC2 and KCC3 are highly homologous, excepting KCC2's extra domain that confers its K^+/Cl^- constitutive transport activity (14,15). The average amino acid sequence identity is even higher within the distal portion of the CTD (see the partial alignment of the last 140 amino acids of potassium-chloride co-transporters in Fig. 1), where the interaction between KCC2 and CK-B has been reported to occur (10). To verify if a specific interaction of KCC3 with CK-B could be detected, we undertook a yeast-two hybrid (Y2H) approach by using a chimerical KCC3 CTD (amino acids 669–1150) construct as the bait. A positive interaction in yeast cells co-transformed with KCC3 and CK-B constructs was identified when cells were grown on selective medium lacking leucine, tryptophan and histidine (–L/W/H) (Fig. 2A). The growth was restricted on this selective medium, compared with the growth on –L/W medium or positive controls grown on –L/W/H medium (data not shown). A weak but discernable β-galactosidase activity was detected by colony lift assay (Fig. 2B). Our results support the hypothesis of an interaction between KCC3 and CK-B in this Y2H system; however, this interaction appears to be restricted, either due to a weak binding between the two proteins or due to properties inherent to the Y2H assay method.

To confirm the interaction between CK-B and KCC3 detected by Y2H assay, we subsequently performed an *in vitro* binding assay using the glutathione S-transferase (GST) fusion protein affinity binding method, which allows the highly sensitive identification of binding partners by subsequent protein sequencing. For the GST pull-down assay, we fused the whole CTD of KCC3 in frame with a GST epitope and expressed the chimeric fusion protein in the presence of 1 mM IPTG (Fig. 3A). Since CK-B is strongly expressed in the nervous system, as detected in Figure 3B and reported by others (16), immobilized GST-tagged KCC3 CTD proteins were incubated with a total protein extract from mouse brain. The resulting protein complexes (Fig. 3C) were identified by LC-MSMS analysis, which showed that GST-CTD co-precipitates with the endogenously expressed CK-B (Fig. 3D). These results strongly support the specificity of the interaction between KCC3 and CK-B.

Wild-type KCC3 co-localizes with CK-B *in vivo* and *in vitro*

Pearson *et al.* (17) and Tachikawa *et al.* (16) have determined that KCC3 and CK-B (Fig. 3B) are both endogenously expressed in the mouse brain at important levels; therefore, using dual-fluorescence immunohistochemical assays, we ascertained the cellular co-expression of endogenous KCC3 and CK-B in adult mouse brain. We found that co-localization of the two proteins was especially strong in cells of the hippocampus and the corpus callosum (Fig. 4A).

To further characterize the interaction between these two proteins, we transfected HeLa cells with a construct bearing the full-length *KCC3* cDNA. Adequate expression of transfected KCC3 and endogenous CK-B was confirmed by Western blot (Fig. 4B and C). Using immunofluorescence labeling, we determined that, as expected, overexpressed KCC3 exhibited a membranous localization, with occasional intracellular localization. The interest of using HeLa cells in this study lies on the fact that they not only have a relatively low endogenous KCC3 expression, as detected by Western blot (Fig. 4B) and by immunofluorescence labeling of non-transfected cells (Fig. 4D), but these commonly used cells also express CK-B endogenously. Using dual-immunofluorescence labeling for KCC3 and CK-B, we observed that overexpressed KCC3 and endogenous CK-B co-localize in HeLa cells: the fluorescence patterns of CK-B and KCC3 substantially overlapped at the cell periphery (Fig. 4D).

The KCC3 region of interaction with CK-B lies in the distal 140 amino acids of the co-transporter's CTD

Since the CTD is the region that mediates KCC3's binding to CK-B, we next attempted to determine the impact on this interaction of the least deleterious of the HMSN/ACC-associated KCC3 CTD truncation mutations. Most of the inherited nonsense mutations so far identified in the *KCC3* gene lie upstream of the CTD and result in the total loss of the CTD.

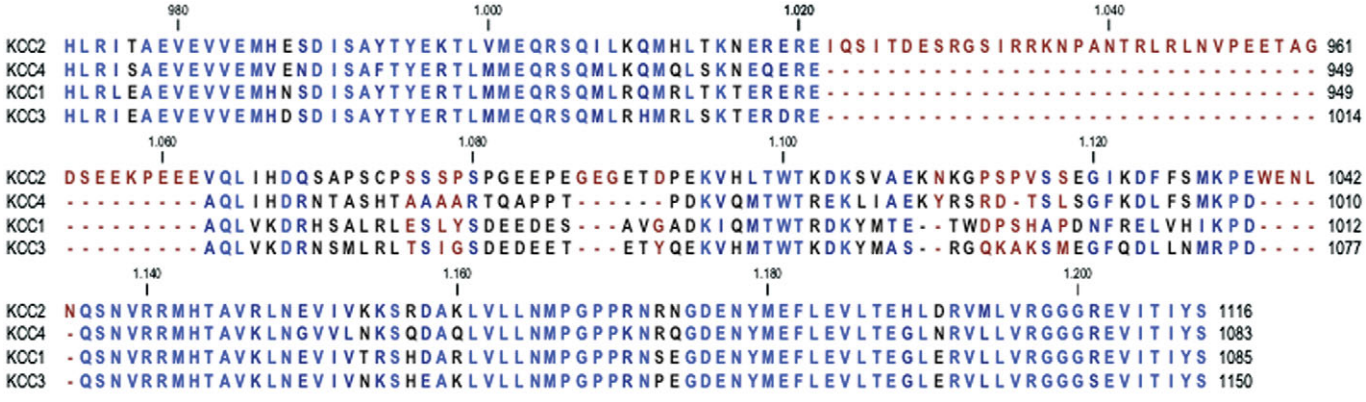

Figure 1. The sequence analysis and conservation of the most distal 140 amino acids of KCC3. The non-conserved residues are indicated in red. The different shades of blue correspond to different levels of conservation between the different KCCs (the lighter the shade of blue, the higher the conservation).

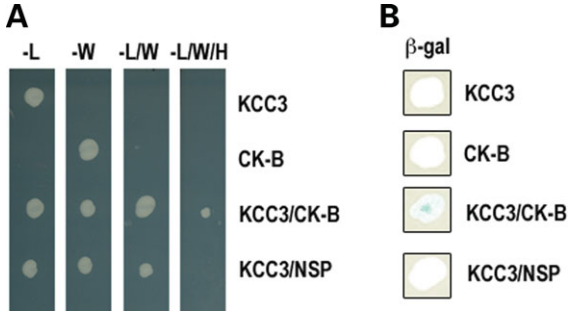

Figure 2. Y2H evidence of interaction between CK-B and the CTD of KCC3. (**A**) CK-B interacts with KCC3's CTD in Y2H experiments. The third column shows growth of co-transformants on medium lacking tryptophane and leucine (−L/W) to select for the presence of both bait and prey vectors. The positive interaction was revealed by the growth of the colonies on medium lacking tryptophane, leucine and histidine (−L/W/H), which requires the activation of the His reporter gene for the acquisition of histidine auxotrophy. (**B**) β-galactosidase assay confirms the Y2H interaction. Yeast cells were transferred to filters and tested for activation of the β-galactosidase reporter gene. Co-transformed yeast cells containing KCC3 and a non-specific prey protein (NSP) show absence of blue coloration upon β-galactosidase assay, whereas cells containing KCC3's CTD and CK-B show a positive but weak β-galactosidase activity. The whole CTD of human KCC3 (amino acids 669–1150; KCC3 in the figure) was used as the 'bait' protein while human CK-B was used as 'prey'.

However, we have recently characterized a less deleterious truncation, R1011X, which results in the loss of less than a third of the CTD (the most distal 140 amino acids of KCC3), which leads to the loss of function of the co-transporter (9). Therefore we tested the ability of the smallest KCC3 amino acid fragment whose loss is known to cause HMSN/ACC to interact with CK-B in Y2H system. For this purpose, the whole CTD of human KCC3 (amino acids 669–1150; CTD in the Figure) and the last 140 amino acids (140-CTD) were used as 'bait' proteins, while human CK-B was used as 'prey'. We found a positive interaction between both CTD fragments and CK-B (Fig. 5A). This result implies that the specific site of interaction between KCC3 and CK-B lies within the last 140 amino acids of KCC3's CTD, suggesting that all HMSN/ACC truncation mutations identified so far necessarily lead to the loss of the interaction with CK-B. We further tested the capacity of smaller distal fragments of KCC3 to interact with CK-B by Y2H, and determined the precise localization of the CK-B binding site to be within the last 18 amino acids of KCC3's CTD (Fig. 5B and Supplementary Material, Figure S).

Loss of co-localization of truncated KCC3 and CK-B implies an impaired interaction between the two proteins

The ability of CK-B to bind KCC3's CTD and the fact that the loss of the CTD (or segments of it) leads to HMSN/ACC, suggest that the disruption of this interaction could play a crucial role in disease pathogenesis. To further investigate the impact of the HMSN/ACC-associated C-terminal R1011X mutation on KCC3's interaction with CK-B, we used dual-immunofluorescence labeling of HeLa cells transfected with the mutant form of KCC3 (R1011X) lacking the last 140 amino acids. In contrast to what was observed for wild-type KCC3, we observed that truncated KCC3 is almost completely retained in the cytoplasm of transfected HeLa cells (Fig. 5D). Furthermore, the co-localization of the co-transporter and CK-B seen for wild-type KCC3 is lost in the R1011X mutant (Fig. 5D). This finding confirms that the HMSN/ACC-associated truncation abrogates the interaction of the mutant co-transporter with its natural partner, CK-B.

Inhibition of CK-B blocks KCC3's activity in a *Xenopus laevis* oocyte flux assay

To ascertain the nature of the interaction between KCC3 and CK-B at a functional level, a flux assay was developed that monitored ion transport triggered by KCC3's activation upon hypotonic stimulation. For this, wild-type KCC3 was expressed in *Xenopus laevis* oocytes (Fig. 6A) and the flux of $^{86}Rb^{+}$ across the plasma membrane was measured as a marker of KCC3 activity; the specificity of the transport was confirmed in parallel by using 1 mM furosemide (from

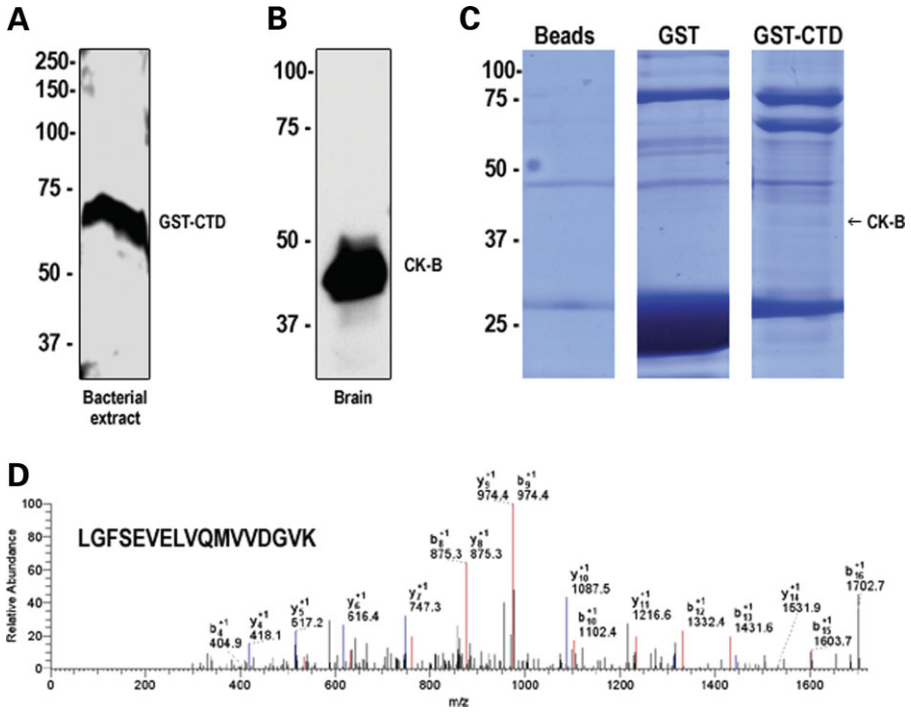

Figure 3. Evidence of interaction between endogenously expressed CK-B and the CTD of KCC3 by GST pull-down. (**A**) Assessment of GST-KCC3 CTD *in vitro* expression. The column corresponds to *E. coli* extract expressing GST-tagged CTD of KCC3 and adequate expression was visualized with an anti-GST antibody. (**B**) Assessment of the endogenous expression of CK-B in the brain. The panel corresponds to a total mouse brain extract and the expression of CK-B is revealed by a specific anti-CK-B antibody. (**C**) Detection of GST pulled-down complexes. Glutathione-sepharose beads, GST only or the fusion protein were incubated with the total mouse brain extract, which contains endogenously expressed CK-B. The resultant bound proteins were revealed on an SDS-page gel with co-omassie blue. Molecular weight markers (in kDa) are shown. (**D**) Identification of CKB protein by LC-MS/MS. MS^2 spectra of a CK-B peptide (each labeled peak corresponds to an amino acid of an internal peptide sequence of CK-B: LGFSEVELVQMVVDGVK). The red peaks indicate matched b-ion series, the blue peaks indicate matched y-ion series and the black peaks indicate unmatched ions. A majority of peaks are matched in agreement with a high cross-correlation score and correspond to mouse CK-B.

2618 ± 325 to 832 ± 99 pmol/oocyte/45 min; ANOVA $P < 0.0005$), an efficient cation-chloride co-transporter inhibitor. In order to evaluate the impact of creatine kinase on KCC3 activity, KCC3-injected oocytes were subsequently incubated with 50 μM of 2,4-Di-Nitro Fluoro Benzene (DNFB), which was reported as a 'fairly good' creatine kinase inhibitor (11,12). In these conditions, the $^{86}Rb^+$ flux was shown to be inhibited to the same extent as that observed under furosemide inhibition (977 ± 48 pmol/oocyte/45 min; ANOVA $P < 0.0005$), suggesting that DNFB inhibition of endogenous creatine kinases completely abolished KCC3-mediated flux of $^{86}Rb^+$ (Fig. 6B). When co-injected with KCC3's RNA, exogenous CK-B did not enhance the $^{86}Rb^+$ uptake, but prevented the flux from being fully inhibited at a low concentration of DNFB (50 μM). Instead, an inhibitor concentration of 200 μM (4-fold) was required for significant inhibition of KCC3-mediated flux of $^{86}Rb^+$, when KCC3 and CK-B were co-injected (Fig. 6C). These data imply that CK-B is required for the activation of KCC3 and suggest a functional interaction between the two proteins.

DISCUSSION

The present study demonstrates that KCC3 physically and functionally interacts with CK-B, an enzyme essential for the generation of ATP. To document the physical interaction between these proteins, we used a variety of approaches, including Y2H system, GST pull-down and immunofluorescence co-localization. Using the Y2H system, we further demonstrated that KCC3's site of binding to CK-B lies within the last 18 amino acids of the transporter, a domain that is lost in all HMSN/ACC-associated truncation mutations. As a result of HMSN/ACC truncation, CK-B's co-localization with KCC3 is no longer observed in immunofluorescence studies. Finally, we used the inhibitory action of DNFB to reveal the crucial role of CK-B activity upon the function of KCC3.

The detection of a physical interaction between KCC3 and CK-B is in agreement with a previous report of a direct interaction between KCC2 and CK-B. However, our observations of a weak *in vitro* interaction between the two proteins suggest that KCC3 and CK-B may interact mainly in a transient manner. Indeed, we failed to efficiently co-immunoprecipitate the two proteins (data not shown), even though we could observe protein co-localization by double immunofluorescence on fixed KCC3-transfected HeLa cells. To further support this observation of a KCC3/CK-B interaction, we observed that the least deleterious HMSN/ACC-associated truncation mutation abolishes the interaction between the two proteins. Even though CK-B is a cytosolic protein, its association with membrane proteins has been repeatedly demonstrated, its

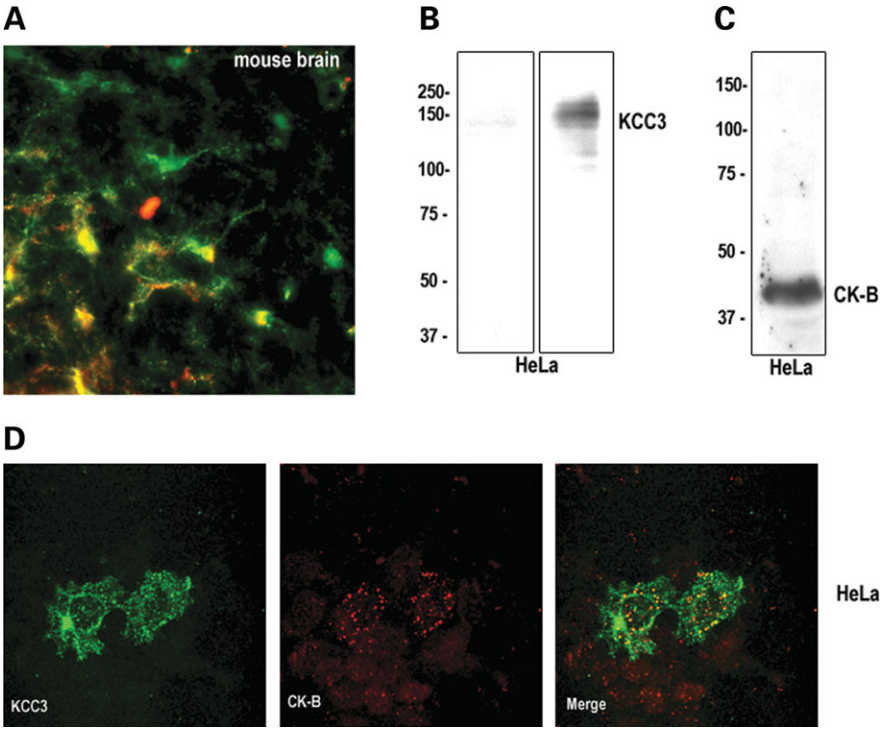

Figure 4. KCC3 and CK-B co-localization. (**A**) Co-expression of endogenously expressed KCC3 (in green) and CK-B (in red) in cells of the mouse brain revealed by immunofluorescence using specific antibodies. (**B**) Western blot analysis of KCC3 in transfected HeLa cells: the first lane shows the endogenous expression of KCC3 in mock-transfected cells and the second lane shows adequate KCC3 expression in the transiently transfected cells, using a specific anti-KCC3 antibody. (**C**) Western blot analysis of CK-B in transfected HeLa cells: the column shows the expression of endogenously expressed CK-B. (**D**) Confocal microscopy observation of CK-B and KCC3 co-localization in HeLa cells. Localization of endogenous CK-B and transiently transfected wild-type KCC3 in HeLa cells revealed by double-immunofluorescence using specific anti-CK-B (in red) and anti-KCC3 (in green) antibodies. Yellow staining corresponds to the co-localization of the two proteins.

interactors including receptors (thrombin receptor, PAR-1; 18) or channels (ATP-sensitive K+ channel; 19). Therefore, as a membrane- associated protein, CK-B is considered to be important for producing the ATP required for ion-driving protein activity. These results are consistent with a previous study showing the requirement of creatine kinase for swelling-activated potassium-chloride co-transport in red blood cells (12). However, the functional significance of the interaction between KCC3 and CK-B remains unclear and the action of ATP on the potassium-chloride co-transporters' function is very complex. Other groups have either demonstrated an ATP-induced activation of KCCs (20,21), or have documented that a decrease in ATP levels and the related Mg^{2+} depletion effect was linked to KCC's activation, although ATP was required for the full stimulation of the co-transporters (22), making this a controversial aspect of KCC3's regulation. We show here that CK-B activity is required for the proper functioning of KCC3, which further supports the hypothesis that ATP is necessary for KCC3 activation. Interestingly, the activity of KCC proteins seems to be modulated by phosphorylation involving kinases and phosphatases (23,24). CK-B's role could, therefore, be to provide the necessary ATP to specific kinases, which in turn would physically interact with KCC3. Alternatively, CK-B itself could be responsible for the direct phosphorylation of KCC3 (25).

The swelling-regulation machinery depends on intracellular and extracellular ATP availability (26,27). It was shown that ATP removal by apyrase inhibits cell volume restoration under hypotonic stress in several cell types (i.e. astrocytes, hepatocytes, airway and intestinal cells and pancreatic acinar cells) (28–31). Hypotonic-swelling stimulates the release of extracellular ATP, which then acts as an autocrinic/paracrinic factor to increase membrane permeability to ions and osmolites (27,32). The action of ATP is ultimately to decrease the cell volume (33). More specifically, it has been reported that in the nervous system an astrocytic ATP release allows a paracrinic signaling to neurons, which are known to have low CK-B, leading to a reduction of the neuronal volume (34,35). In addition, the characteristics of necrotic swelling of nerve cells include a deleterious volume increase of the cells associated with a rapid ATP depletion (36). Given the central role of ATP in nerve cell volume regulation, ATP trafficking is likely to play a key role in controlling cell volume decrease in the nervous system.

Solute carriers, along with volume-regulated channels, control the responses involved in cell volume regulation and ion distribution. Among the members of the SLC12 family of proteins, NKCC1 and KCC2 seem to play the most pivotal roles in both neuronal development and functioning (4), but neither one of them is involved in the RVD response in neurons. In contrast, KCC3 is activated under hypotonic conditions to induce the RVD response, which is greatly impaired in HMSN/ACC patients (2,9). Volume adaptation to osmotic stress and management of ion distribution are

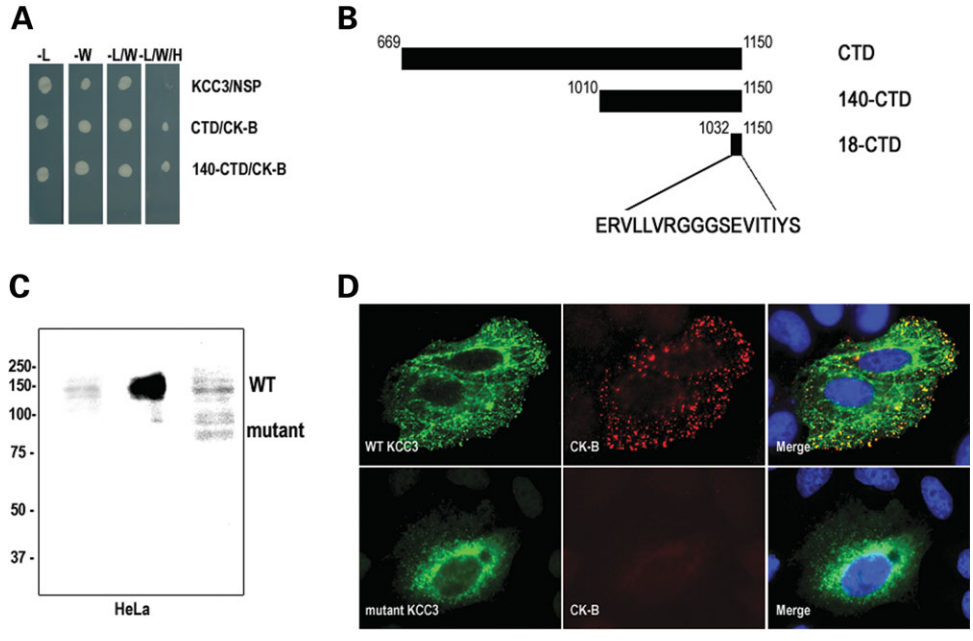

Figure 5. Impairment of CK-B's interaction with KCC3 by HMSN/ACC KCC3 truncating mutations. (**A**) Whole (amino acids 669–1150) and distal (amino acids 1011–1150) regions of human KCC3 CTD were used as baits in the Y2H assay. Human CK-B was used as the prey protein. The interaction between CK-B and both CTD fragments was revealed by the acquisition of histidine auxotrophy of the transformed yeast cells grown on media lacking tryptophane, leucine and histidine (–L/W/H). (**B**) Schematic diagram representing C-terminal fragments of KCC3 used in the yeast two-hybrid experiments. (**C**) Western blot analysis confirms expression of wild-type (middle lane) and truncated KCC3 (right lane) in transiently transfected HeLa cells. Western blot of the mock-transfected HeLa cells is shown on the left lane. The upper bands, seen above the truncated KCC3, correspond to the endogenously expressed KCC3 in HeLa cells. (**D**) Comparison of co-localization of CK-B with wild-type (upper panels) or mutant R1011X (lower panels) KCC3 forms in transiently transfected HeLa cells. Double immunofluorescent labeling of KCC3 (green) and CK-B (red) shows a loss of co-localization of the truncated KCC3 and CK-B.

primary or secondary active mechanisms that are highly energy-demanding. In nerve and glial cells, because of their distinctive shape and of the constant intracellular and environmental challenges in ion distribution, energy requirements need to be fine-tuned to an even greater extent. An important amount of energy is also required during nervous system development, given the tasks of elongating and orienting axons, while correct myelin ensheathment occurs. Therefore, an adequate energy supply is of crucial importance for osmotic-dependant integrity of neurons, but is also essential for the proper development of the nervous system. Taking all these observations together, a potential prominent role emerges for the interaction of KCC3 with CK-B, which, when abrogated, could be a major contributor to the neurological defects observed in HMSN/ACC patients. The elucidation and characterization of this protein–protein interaction could, therefore, lead to the better understanding of the pathological mechanisms of HMSN/ACC and ultimately lead to the development of therapies and improved patient management.

MATERIALS AND METHODS

Constructs

The construct containing the full-length KCC3 cDNA in the pGEM vector was kindly provided by Dr David Mount (Harvard Medical School, Boston, MA, USA). To allow the expression of KCC3 protein in mammalian cells, the full-length cDNA in pGEM was digested with Sac*II* and EcoR*I* and subcloned into the pcDNA 3.1C vector (Invitrogen). Site-directed mutagenesis was performed using appropriate primers to produce the 3031C→T transition, which is the least deleterious KCC3 truncation characterized so far (R1011X mutant protein). The whole KCC3 CTD was amplified using 5′-GGATCCGTCGACTCGATGGTATCCGTGGG CTGGT-3′ and 5′-ATGCGGCCGCTCTAGAGAATTCAGAG TAGGTTAT-3′ primers, containing BamH*I* and Not*I* cloning sites in-frame. The PCR fragment was purified, restriction enzyme-digested with BamH*I* and Not*I* and cloned into the corresponding sites in the pGEX 3T-1 vector (Amersham), which allows the production of GST-fused proteins.

For Y2H experiments, CK-B cDNA was purchased from MGC library (IMAGE: 4135106) and Gateway recombination cloning system-compatible primers (5′-CACCATGCCCTTC TCCAACAGCCATAATACGCAG-3′ and 5′-CTTCTGGG CCGGCATGAGGTCATCGATTGC-3′) were used to amplify the cDNA. KCC3's whole CTD sequence and distal CTD sequence coding for the last 140 amino acids of KCC3 were amplified using appropriate Gateway recombination cloning system-compatible primers (5′-CACCGAGGCACAA TTGGTGAAAG-3′ and 5′-CTTCTGGGCCGGCATGAGGT CATCGATTGC-3′ respectively). The CK-B and KCC3 PCR products were first cloned into the pENTR entry vector (Invitrogen) and sequence accuracy was confirmed by sequencing. The CK-B fragment was then subcloned into the Gateway-compatible vector pDEST-22 containing a 3′-*GAL4* activation domain, and KCC3′s fragments were subcloned into pDEST-32, which contains 3′-*GAL4* DNA binding

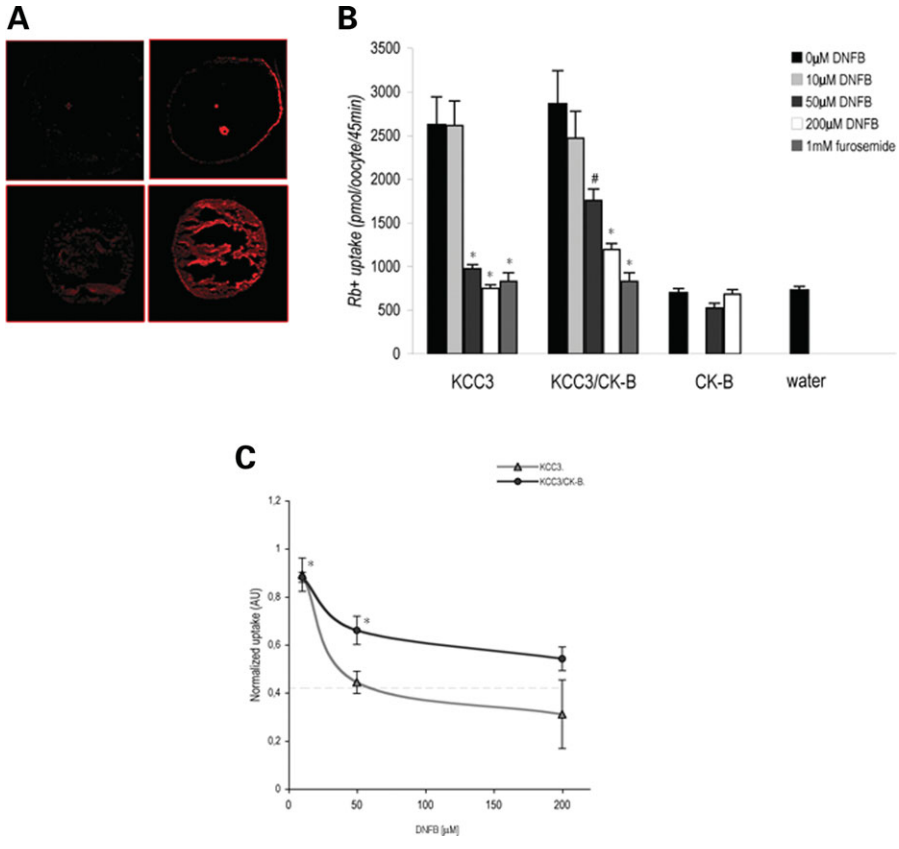

Figure 6. Functional impact of CK-B's interaction with KCC3 in *Xenopus laevis* oocyte flux assay. (**A**) Immunofluorescent analysis of KCC3 availability at the membrane of *Xenopus laevis* oocytes (16× magnification). KCC3 immunostaining of 10 μm-thick cryosections of: a water-injected oocyte as a control, stained with anti-CK-B antibody (upper-left panel), a water-injected oocyte stained with anti-KCC3 antibody (lower-left panel), a KCC3-injected oocyte stained with anti-KCC3 antibody (upper-right panel) and a CK-B-injected oocyte stained with anti-CK-B antibody (lower-right panel) (each representative of 10 stainings). Note that anti-CK-B antibody raised against the human form shows low affinity for CK-B endogenously expressed in *Xenopus laevis*. (**B**) Assessment of KCC3's flux dependant of CK-B activity. Measurements of $^{86}Rb^{+}$ uptake invoked under hypotonic conditions in a representative experiment in *Xenopus laevis* oocytes injected with the wild-type KCC3 cRNA alone, wild-type KCC3 and exogenous CK-B, CK-B cRNA alone or water. All of the values shown are expressed as mean flux rates ± S.E. of 13–21 oocytes and * indicates that the corresponding value is significantly different ($P < 0.01$) relative to flux rates of KCC3 without inhibitor; # indicates a moderate significance ($0.05 < P < 0.01$). Wild-type KCC3 activation mediated a significant $^{86}Rb^{+}$ transport, which was fully abolished by 1 mM furosemide, as well as by 50 μM of DNFB, a specific inhibitor of CK-B. Note that 200 μM DNFB did not affect the intracellular distribution of wild-type KCC3 in the immunofluorescence studies of Figure 5D. (**C**) Quantitative assessment of CK-B's protective effect over the DNFB-dependant inhibition of KCC3 activity. The values shown are normalized with the flux rates without DNFB ± SE of 12–25 oocytes among four to seven different experiments, and * indicates that the corresponding value is significantly different ($P < 0.01$) relative to the KCC3+1 mM furosemide value. The mean value of KCC3+1 mM furosemide flux rate is indicated by a dashed line. Fifty microlitter of DNFB was sufficient to significantly inhibit the KCC3-driven furosemide-sensitive flux of $^{86}Rb^{+}$. A minimum of 200 μM of DNFB was required to abolish KCC3's activity when CK-B was co-overexpressed in the oocytes.

domain. Subcloning by recombination with LR-recombinase (Invitrogen) was performed according to the manufacturer's instructions.

Yeast two-hybrid

Chemically competent yeast MaV203 cells (*MATα; leu2-3,112; trp1-901; his3Δ200; ade2-101*; *cyh2R; can1R; gal4Δ; gal80Δ; GAL1::lacZ; HIS3UASGAL1::HIS3@LYS2; SPAL10::URA3*) were co-transformed with the bait plasmid, which carried the *LEU2* marker, and the prey plasmid carrying the *TRP1* marker. No self-activation of the bait and the prey strain reporter genes was obtained on synthetic drop-out (SD)−Ura/His medium. Transformed yeast cells were grown on SD−Leu/Trp plates for selection of co-transformed cells. Colonies were picked onto SD−Leu/Trp/His plates for assessment of interactions. Activation of the LacZ reporter was assayed by growing the yeast on filter paper on YPAD plates overnight, lysing the cells in liquid nitrogen and then incubating the filter papers at 37°C for 1 h on filters pre-soaked in 100 μl 10% X-gal, 60 μl β-mercaptoethanol and 10 ml Z buffer (100 mM Na_2HPO_4, 40 mM NaH_2PO_4, 10 mM KCl, 1 mM $MgSO_4$, pH 7).

In vitro binding assay

The CTD of KCC3 cloned in pGEX was propagated in the bacterial strain BL21. A single colony was incubated in 3 ml of LB (containing 100 μg/ml ampicillin), grown overnight at 37°C and used to produce large-scale cultures. Large-scale cultures were grown until $OD_{600nm} = 0.6–0.8$ at 30°C and incubated with 0.1 mM IPTG for an additional 30 min to 2 h

at 30°C. The expression of the fusion protein was assessed by Western blot using a GST-specific antibody. The fusion protein was purified using standard procedures with 500 μl of 50% slurry glutathione-sepharose beads (Amersham). The binding assays were performed for 1 h at 4°C in 500 μl of binding solution containing a total brain protein extract, under rocking movement. Following incubation, the beads were rinsed three times for 1 h at 4°C in a modified RIPA buffer and carefully drained. The dried beads containing the bound complexes were sent to Wemb Biochem Inc. (Toronto) for protein sequencing using an LC-MS protocol. In parallel, the beads containing the purified complexes were dissociated by boiling for 10 min in sample buffer. The unbound complexes were finally loaded on an SDS–PAGE gel and stained with coomassie blue to assess protein integrity.

Antibodies

Monoclonal anti-GST primary antibody was obtained from Clontech. Monoclonal and polyclonal anti-CK-B primary antibodies were obtained from OEM concept. Polyclonal anti-KCC3 primary antibody, which recognizes the N-terminal domain of the transporter, was obtained from Abnova. Peroxidase-conjugated secondary antibodies for Western blotting were obtained from the Jackson Labs. Secondary antibodies for immunofluorescence were obtained from the Jackson Labs.

HeLa cell transfection and immunocytochemistry

HeLa cells were seeded on sterile plastic coverslips in six-well plates and transfected with 4 μg of full-length KCC3 or R1011X vector DNA using lipofectamine 2000 (Invitrogen), according to the manufacturer's instructions. Following transfection, cells were incubated for 24 h in Dulbecco's modified Eagle's medium (DMEM, GIBCO) containing 10% fetal bovine serum, then washed in PBS and fixed in 4% paraformaldehyde in PBS at room temperature for 10 min. Fixed cells were washed in PBS before being permeabilized in PBS containing 0.2% Triton X-100 (Sigma) at room temperature for 10 min. Permeabilized cells were then washed in PBS, incubated for 1 h in blocking solution (10% NGS in PBS) and transferred to a 5% NGS in PBS solution containing anti-CK-B (OEM concept) and anti-KCC3 (Abnova) antibodies at an appropriate dilution (1:100 and 1:200, respectively). After an overnight incubation, coverslips were washed in PBS and were then incubated for 60 min in 5% NGS in PBS containing fluorescent secondary antibodies. The coverslips were finally washed in PBS and mounted for fluorescent microscopy or confocal visualization.

Mouse brain preparation and immunohistochemistry

Mouse brains fixed in 4% paraformaldehyde were embedded in Tissue-Tek, sectioned parasagitally (10 μm) and placed on glass slides. The sections were processed for immunohistochemistry using a standard in-house protocol (37). After permeabilization and blocking steps, the sections were incubated overnight in 5% NGS in PBS containing anti-KCC3 and anti-CK-B antibodies (1:150 and 1:200, respectively) and revealed by a 1 h incubation with fluorescent secondary antibodies, followed by slide mounting for confocal microscopy.

Flux assay

In vitro *cRNA transcription*. The pGEM templates were linearized downstream from the 3′-end of the coding sequence with Not*I*, and the cRNAs were transcribed *in vitro* using T7 RNA polymerase. Transcript integrity was verified on agarose gels, and concentration was evaluated by absorbance reading at 280 nm and by the densitometric analysis of the corresponding band in ethidium bromide-stained gels.

Xenopus laevis *oocyte preparation*. *Xenopus laevis* oocytes were surgically harvested from anesthetized adult female animals and defolliculated at room temperature for 2 h with 2 mg/ml collagenase A. Stage V and VI healthy oocytes were injected with 50 nl of water with or without cRNA (total KCC3 cRNA injected was 10 ng/oocyte and total CK-B cRNA injected was 4.6 ng/oocyte). After injection, oocytes were incubated at 18°C for 5 days in Barth's solution (90 mM NaCl, 3 mM KCl, 0.82 mM $MgCl_2$, 0.74 mM $CaCl_2$, 10 mM HEPES/Tris, 5% (v/v) horse serum, pH 7.6) to allow for recovery and protein expression.

Assessment of KCC3 function. The activity of KCC3 was determined by assessing $^{86}Rb^+$ uptake in groups of 20 oocytes or more. The uptake was measured at 32°C using a standard protocol: a 60 min incubation period in a hypototonic medium (52 mM Na-Cyclamate, 3.3 mM KCl, 0.74 mM $CaCl_2$, 0.82 mM $MgCl_2$, 10 mM HEPES/Tris, pH 7.4) with 10 μM ouabain, was followed by incubation in an uptake medium containing 49 mM NaCl, 15 mM Na-Cyclamate, 0.74 mM $CaCl_2$, 0.82 mM $MgCl_2$, 10 mM HEPES/Tris, pH 7.4, 5 mM $^{86}Rb^+$-Cl^- and 10 μM ouabain. The KCC3- dependant uptake of $^{86}Rb^+$ was deduced by exposing groups of cRNA-injected oocytes to 1 mM furosemide. The CKB-dependant uptake was deduced by exposition to 50–200 μM of 2,4-Di-Nitro Fluoro Benzene (DNFB). The uptake experiment was stopped after 45 min by five washes in ice-cold uptake solution without the isotope, to remove extracellular fluid tracer. The oocytes were lysed in 10% sodium dodecyl sulfate and tracer activity was measured for 2 min in a liquid scintillation counter.

Statistical analysis. Statistical significance was defined as $P < 0.01$, and the results were presented as means ± SE. The significance of the differences between oocyte groups was tested by one-way ANOVA and two-tailed Student *t*-test.

SUPPLEMENTARY MATERIAL

Supplementary Material is available at HMG Online.

Conflict of Interest statement. The authors have reported no conflicts of interest.

FUNDING

This work was supported by the Canadian Institutes of Health Research (CIHR grant no. 172248) and the 'Fondation des jumelles Coudé'.

REFERENCES

1. Dupre, N., Howard, H.C., Mathieu, J., Karpati, G., Vanasse, M., Bouchard, J.P., Carpenter, S. and Rouleau, G.A. (2003) Hereditary motor and sensory neuropathy with agenesis of the corpus callosum. *Ann. Neurol.*, **54**, 9–18.
2. Howard, H.C., Mount, D.B., Rochefort, D., Byun, N., Dupre, N., Lu, J., Fan, X., Song, L., Riviere, J.B., Prevost, C. *et al.* (2002) The K-Cl cotransporter KCC3 is mutant in a severe peripheral neuropathy associated with agenesis of the corpus callosum. *Nat. Genet.*, **32**, 384–392.
3. Mount, D.B., Mercado, A., Song, L., Xu, J., George, A.L., Jr, Delpire, E. and Gamba, G. (1999) Cloning and characterization of KCC3 and KCC4, new members of the cation-chloride cotransporter gene family. *J. Biol. Chem.*, **274**, 16355–16362.
4. Hebert, S.C., Mount, D.B. and Gamba, G. (2004) Molecular physiology of cation-coupled Cl^- cotransport: the SLC12 family. *Pflugers Arch.*, **447**, 580–593.
5. Hiki, K., D'Andrea, R.J., Furze, J., Crawford, J., Woollatt, E., Sutherland, G.R., Vadas, M.A. and Gamble, J.R. (1999) Cloning, characterization, and chromosomal location of a novel human K^+-Cl^- cotransporter. *J. Biol. Chem.*, **274**, 10661–10667.
6. Mercado, A., Vazquez, N., Song, L., Cortes, R., Enck, A.H., Welch, R., Delpire, E., Gamba, G. and Mount, D.B. (2005) NH2-terminal heterogeneity in the KCC3 K+-Cl^- cotransporter. *Am. J. Physiol. Renal Physiol.*, **289**, F1246–F1261.
7. Race, J.E., Makhlouf, F.N., Logue, P.J., Wilson, F.H., Dunham, P.B. and Holtzman, E.J. (1999) Molecular cloning and functional characterization of KCC3, a new K-Cl cotransporter. *Am. J. Physiol.*, **277**, C1210–C1219.
8. Uyanik, G., Elcioglu, N., Penzien, J., Gross, C., Yilmaz, Y., Olmez, A., Demir, E., Wahl, D., Scheglmann, K., Winner, B. *et al.* (2006) Novel truncating and missense mutations of the KCC3 gene associated with Andermann syndrome. *Neurology*, **66**, 1044–1048.
9. Salin-Cantegrel, A., Riviere, J.B., Dupre, N., Charron, F.M., Shekarabi, M., Karemera, L., Gaspar, C., Horst, J., Tekin, M., Deda, G. *et al.* (2007) Distal truncation of KCC3 in non-French Canadian HMSN/ACC families. *Neurology*, **69**, 1350–1355.
10. Inoue, K., Ueno, S. and Fukuda, A. (2004) Interaction of neuron-specific K+-Cl^- cotransporter, KCC2, with brain-type creatine kinase. *FEBS Lett.*, **564**, 131–135.
11. Inoue, K., Yamada, J., Ueno, S. and Fukuda, A. (2006) Brain-type creatine kinase activates neuron-specific K+-Cl^- co-transporter KCC2. *J. Neurochem.*, **96**, 598–608.
12. Colclasure, G.C., Parker, J.C. and Dunham, P.B. (1995) Creatine kinase is required for swelling-activated K-Cl cotransport in dog red blood cells. *Am. J. Physiol.*, **268**, 660–668.
13. Wyss, M. and Kaddurah-Daouk, R. (2000) Creatine and creatinine metabolism. *Physiol. Rev.*, **80**, 1107–1213.
14. Song, L., Mercado, A., Vazquez, N., Xie, Q., Desai, R., George, A.L., Jr, Gamba, G. and Mount, D.B. (2002) Molecular, functional, and genomic characterization of human KCC2, the neuronal K-Cl cotransporter. *Brain Res. Mol. Brain Res.*, **103**, 91–105.
15. Mercado, A., Broumand, V., Zandi-Nejad, K., Enck, A.H. and Mount, D.B. (2006) A C-terminal domain in KCC2 confers constitutive K+-Cl^- cotransport. *J. Biol. Chem.*, **281**, 1016–1026.
16. Tachikawa, M., Fukaya, M., Terasaki, T., Ohtsuki, S. and Watanabe, M. (2004) Distinct cellular expressions of creatine synthetic enzyme GAMT and creatine kinases uCK-Mi and CK-B suggest a novel neuron-glial relationship for brain energy homeostasis. *Eur. J. Neurosci.*, **20**, 144–160.
17. Pearson, M.M., Lu, J., Mount, D.B. and Delpire, E. (2001) Localization of the K(+)-Cl(-) cotransporter, KCC3, in the central and peripheral nervous systems: expression in the choroid plexus, large neurons and white matter tracts. *Neuroscience*, **103**, 481–491.
18. Mahajan, V.B., Pai, K.S., Lau, A. and Cunningham, D.D. (2000) Creatine kinase, an ATP-generating enzyme, is required for thrombin receptor signaling to the cytoskeleton. *Proc. Natl Acad. Sci. USA*, **97**, 12062–12067.
19. Crawford, R.M., Ranki, H.J., Botting, C.H., Budas, G.R. and Jovanovic, A. (2002) Creatine kinase is physically associated with the cardiac ATP-sensitive K+ channel in vivo. *FASEB J.*, **16**, 102–104.
20. Lauf, P.K. (1983) Thiol-dependent passive K+-Cl^- transport in sheep red blood cells. V. Dependence on metabolism. *Am. J. Physiol.*, **245**, C445–C448.
21. Lauf, P.K., Bauer, J., Adragna, N.C., Fujise, H., Zade-Oppen, A.M., Ryu, K.H. and Delpire, E. (1992) Erythrocyte K-Cl cotransport: properties and regulation. *Am. J. Physiol.*, **263**, C917–C932.
22. Ortiz-Carranza, O., Adragna, N.C. and Lauf, P.K. (1996) Modulation of K-Cl cotransport in volume-clamped low-K sheep erythrocytes by pH, magnesium, and ATP. *Am. J. Physiol.*, **271**, C1049–C1058.
23. Adragna, N.C., Di Fulvio, M. and Lauf, P.K. (2004) Regulation of K-Cl cotransport: from function to genes. *J. Membr. Biol.*, **201**, 109–137.
24. Bergeron, M.J., Gagnon, E., Caron, L. and Isenring, P. (2006) Identification of key functional domains in the C terminus of the K+-Cl^- cotransporters. *J. Biol. Chem.*, **281**, 15959–15969.
25. Hemmer, W., Furter-Graves, E.M., Frank, G., Wallimann, T. and Furter, R. (1995) Autophosphorylation of creatine kinase: characterization and identification of a specifically phosphorylated peptide. *Biochim. Biophys. Acta*, **1251**, 81–90.
26. Wang, Y., Roman, R., Lidofsky, S.D. and Fitz, J.G. (1996) Autocrine signaling through ATP release represents a novel mechanism for cell volume regulation. *Proc. Natl Acad. Sci. USA*, **93**, 12020–12025.
27. Dubyak, G.R. and el-Moatassim, C. (1993) Signal transduction via P2-purinergic receptors for extracellular ATP and other nucleotides. *Am. J. Physiol.*, **265**, C577–C606.
28. Mongin, A.A. and Kimelberg, H.K. (2005) ATP regulates anion channel-mediated organic osmolyte release from cultured rat astrocytes via multiple Ca2+-sensitive mechanisms. *Am. J. Physiol. Cell. Physiol.*, **288**, C204–C213.
29. Feranchak, A.P., Fitz, J.G. and Roman, R.M. (2000) Volume-sensitive purinergic signaling in human hepatocytes. *J. Hepatol.*, **33**, 174–182.
30. Dezaki, K., Tsumura, T., Maeno, E. and Okada, Y. (2000) Receptor-mediated facilitation of cell volume regulation by swelling-induced ATP release in human epithelial cells. *Jpn J. Physiol.*, **50**, 235–241.
31. Okada, S.F., Nicholas, R.A., Kreda, S.M., Lazarowski, E.R. and Boucher, R.C. (2006) Physiological regulation of ATP release at the apical surface of human airway epithelia. *J. Biol. Chem.*, **281**, 22992–23002.
32. Feranchak, A.P., Roman, R.M., Schwiebert, E.M. and Fitz, J.G. (1998) Phosphatidylinositol 3-kinase contributes to cell volume regulation through effects on ATP release. *J. Biol. Chem.*, **273**, 14906–14911.
33. Franco, R., Panayiotidis, M.I. and de la Paz, L.D. (2008) Autocrine signaling involved in cell volume regulation: the role of released transmitters and plasma membrane receptors. *J. Cell. Physiol.*, **216**, 14–28.
34. Joseph, S.M., Buchakjian, M.R. and Dubyak, G.R. (2003) Colocalization of ATP release sites and ecto-ATPase activity at the extracellular surface of human astrocytes. *J. Biol. Chem.*, **278**, 23331–23342.
35. Queiroz, G., Meyer, D.K., Meyer, A., Starke, K. and von Kugelgen, I. (1999) A study of the mechanism of the release of ATP from rat cortical astroglial cells evoked by activation of glutamate receptors. *Neuroscience*, **91**, 1171–1181.
36. Okada, Y., Maeno, E., Shimizu, T., Dezaki, K., Wang, J. and Morishima, S. (2001) Receptor-mediated control of regulatory volume decrease (RVD) and apoptotic volume decrease (AVD). *J. Physiol.*, **532**, 3–16.
37. Gaspar, C., Jannatipour, M., Dion, P., Laganiere, J., Sequeiros, J., Brais, B. and Rouleau, G.A. (2000) CAG tract of MJD-1 may be prone to frameshifts causing polyalanine accumulation. *Hum. Mol. Genet.*, **9**, 1957–1966.